International Journal of Applied Power Engineering (IJAPE)
Vol. 15, No. 2, June 2026, pp. 942~947
ISSN: 2252-8792, DOI: 10.11591/ijape.v15.i2.pp942-947

Investigation of the photoluminescence properties of quantum dots using theoretical simulation

Le Doan Duy, Le Xuan Thuy
Faculty of Basic Sciences, Vinh Long University of Technology Education, Vinh Long, Vietnam

Article Info

Article history:

Received Jul 21, 2025
Revised Feb 9, 2026
Accepted Mar 12, 2026

Keywords:

Photoluminescence
Quantum confinement
Quantum dots
Recombination
Stokes shift

ABSTRACT

This study investigates the optical behavior of CdSe quantum dots, a class of semiconductor nanomaterials widely studied for light-emitting, photovoltaic, and bioimaging applications owing to their size-dependent electronic structure. The objective is to clarify the relationship between quantum dot size, size distribution, and emission characteristics through experimental and simulated optical spectra. UV–Vis absorption, photoluminescence, and simulated PL spectra were analyzed for CdSe quantum dots excited at 325 nm. The experimental PL spectrum exhibits a single and narrow emission band assigned to the 1Se → 1Sh transition, which is blue-shifted compared with bulk CdSe, confirming strong quantum confinement in 2–3 nm particles with a very narrow size distribution of less than 1%. A large Stokes shift of 0.93 eV is observed, attributed to confinement effects and surface-related states. Simulated photoluminescence (PL) spectra for 3–6 nm quantum dots show progressive red-shifting and spectral broadening with increasing particle size, while smaller quantum dots display stronger PL intensity due to enhanced confinement and more efficient radiative recombination. Parameter analysis further reveals that size deviation and linewidth broaden emission and reduce intensity without changing the peak wavelength. These findings provide useful guidance for optimizing CdSe quantum dots for QLEDs, bioimaging, and broadband optoelectronic devices.

Corresponding Author:

Le Xuan Thuy
Faculty of Basic Sciences, Vinh Long University of Technology Education
Vinh Long, Vietnam
Email: thuylx@vlute.edu.vn

1. INTRODUCTION

Semiconductor nanoparticles exhibit quantum confinement effects on electrons and phonons, which strongly influence their optical and electrical properties [1]. Confinement leads to an increase in the direct interband transition energy, enabling the band gap to be tuned by modifying particle size [2]. A substantial enhancement, by several orders of magnitude, in radiative recombination efficiency has also been reported [3]. The nonlinear dependence of electronic excitation energy on particle size allows semiconductor nanoparticles to be used in applications such as second harmonic generation and long-pass optical filters [4]. However, this nonlinear optical response can be greatly suppressed when the crystallite size is nonuniform. Therefore, determining both the particle size and its distribution is essential.

Commonly, the average size of nanoparticles is estimated using the width of major X-ray diffraction (XRD) peaks via Scherrer's formula. Although widely applied, this method neglects the effects of lattice distortion on peak broadening and does not provide information about size distribution. High-resolution transmission electron microscopy (HRTEM) offers direct measurement of particle size and distribution [5]–[7], but the technique is destructive and requires complex sample preparation.

An alternative approach uses the frequencies of confined acoustic phonons obtained from low-frequency Raman spectra to estimate particle size. Nevertheless, the assignment of vibrational modes can be ambiguous. Moreover, particle size significantly affects optical characteristics, causing inhomogeneous broadening in optical spectra. For example, Jun and Tung [8] calculated the absorption spectrum of quantum dots with a finite size distribution using an infinite-potential-well model that neglects intrinsic linewidth arising from vibronic coupling, resulting in a delta-function spectrum for monodisperse dots.

Efforts to match computed absorption spectra with experimental data have been reported [9], [10], but these require prior knowledge of parameters such as oscillator strength, bandwidth, and the energies of all electronic transitions. For materials like CdSe, up to 12 parameters may be needed, and these values—often approximated from empirical relations or band-structure calculations—can introduce significant uncertainties. In contrast, photoluminescence (PL) spectra typically exhibit distinct features associated with band-edge emission and defect-related recombination [11], [12]. Although the inhomogeneous broadening of these spectra is also linked to particle size distribution, a quantitative analysis has not yet been performed.

This study proposes a simple and robust method for analyzing the inhomogeneously broadened band-edge PL lineshape to extract particle size distribution. The method is validated using the PL spectra of CdSe nanoparticles with diameters ranging from 3 to 6 nm. To reduce the number of fitting parameters, the measured photoluminescence spectrum of bulk CdSe is employed as an input reference for lineshape estimation.

2. METHOD

2.1. Experimental section

During the high-temperature synthesis of CdSe quantum dots, the Cd:OA ratio was fixed at 1:4.1 and Se:TOP at 1:3.23, while varying the Cd:Se ratio, temperature, and reaction time to investigate their effects on particle size and quality. The synthesis procedure is as follows: A mixture of $(CH_3COO)_2Cd{\cdot}2H_2O$, OA, and DPE (as solvent) was stirred and heated at 120–180 °C under a nitrogen atmosphere to form a pale-yellow Cd–OA complex solution. Separately, a 0.1 M Se–TOP solution was prepared and quickly injected into the reaction flask. Within seconds, the solution changed color depending on the reaction conditions. Crystal growth was controlled by maintaining the temperature for a set duration. Particle size was indirectly determined using UV-vis absorption and photoluminescence spectra. To stop the reaction, 6 mL of toluene was rapidly added to cool the mixture. The resulting CdSe QDs were purified by precipitating with methanol, centrifuging at 3000 rpm for 15 minutes, discarding the supernatant, and redispersing the precipitate in toluene. This purification process could be repeated several times.

2.2. Theoretical simulation

The PL spectrum of a direct bandgap semiconductor material with a bandgap energy of E_0 is distributed according to a Gaussian function. Here Γ is the full width at half maximum (FWHM) of the PL spectrum.

$$g_b(E) = \frac{A}{\sqrt{2\pi}\Gamma} exp\left[-\frac{(E-E_0)^2}{2\Gamma^2}\right] \quad (1)$$

We have that E_0 depends on the size of the nanoparticle.

$$E(R_0) = E_0 + \frac{\hbar^2\pi^2}{2R^2}\left[\frac{1}{m_e}+\frac{1}{m_h}\right] - \frac{1.8e^2}{4\pi\varepsilon_0\varepsilon R} + \frac{e^2}{R}\sum\alpha_n \quad (2)$$

Therefore, (1) is rewritten as (3).

$$g_{qd}(E,R_0) = \frac{A}{\sqrt{2\pi}\Gamma} exp\left[-\frac{(E-E(R_0)^2}{2\Gamma^2}\right] \quad (3)$$

On the other hand, the particle sizes are not uniformly distributed, resulting in a particle size distribution that follows a Gaussian distribution function.

$$P(R) = \frac{A}{\sqrt{2\pi}\sigma_R} exp\left[-\frac{(R-R_0)^2}{2{\sigma_R}^2}\right] \quad (4)$$

The σ_R refers to the standard deviation, which is determined through p = σ_R/R_0. The shape of the photoluminescence (PL) spectrum is thus determined by (5).

$$G(E) = \int P(R).g_{qd}(E,R)dR \quad (5)$$

Infer:

$$G(E) = \frac{1}{2\pi\Gamma\sigma_R}\int_0^\infty exp\left[-\frac{(R-R_0)^2}{2\sigma^2} - \frac{(E-E(R))^2}{2\Gamma^2}\right]dR \quad (6)$$

The (6) is the formula we use for simulation, allowing the computer to generate the photoluminescence (PL) spectrum when we input the particle size as a parameter. An approximation of (2) can be made by neglecting the third term.

$$E(R_0) = E_0 + \frac{\hbar^2\pi^2}{2R^2}\left[\frac{1}{m_e} + \frac{1}{m_h}\right] - \frac{1.8e^2}{4\pi\varepsilon_0\varepsilon R} \quad (7)$$

With the CdSe material, we have: E_0 = 1.74 eV, m_e = 0.13 m_0, m_h = 0.4 m_0, and ε = 10.6. The Γ parameter of bulk CdSe is 0.185 eV [13].

$$E(R) = 1.74 + \frac{3.845}{R^2} - \frac{0.4465}{R} \ \text{(eV, nm)} \quad (8)$$

3. RESULTS AND DISCUSSION

Figure 1 displays the UV-Vis absorption spectrum of the FTO/QDs photoanode with ZnS and ZnSe passivation layers doped - Cu^{2+} in the range of 300–700 nm. Light is illuminated from the FTO substrate side, showing absorption dependence on the Cu^{2+} doping ratio. Below 550 nm, the absorption intensity slightly increases with Cu^{2+} content, possibly due to the formation of Cu^{2+} energy levels within the bandgap of ZnS and ZnSe. This result is consistent with the study on Sr doping in ZnSe for QDSSCs [14]. The FTO/TiO_2/QDs/ZnSe@Cu^{2+} system exhibits enhanced absorption and a red shift in the 500–600 nm range. The FTO/TiO_2/QDs/ZnSe@Cu^{2+} photoanode shows a higher absorption spectrum intensity than the FTO/TiO_2/QDs/ZnS@Cu^{2+} photoanode. Overall, the doped anode films absorb longer wavelengths, extend into the visible light region, and result in a darker material.

X-ray diffraction (XRD) analysis was employed to investigate the structural characteristics of CdS, CdSe, ZnS@Cu^{2+}, and ZnSe@Cu^{2+} quantum dots deposited on the TiO_2 surface. The diffraction patterns (Figure 2) confirm the crystalline nature of all samples. Specifically, five prominent diffraction peaks of TiO_2 observed at 25.354°, 37.785°, 48.077°, 53.922°, and 62.728° are indexed to the (101), (004), (200), (105), and (204) planes, respectively, corresponding to the anatase phase (JCPDS No. 00-004-0477) [15]. The cubic phase of CdS is identified by the characteristic (111) and (222) reflections at 26.5° and 54.5°, respectively (JCPDS No. 00-089-0440) [15], [16]. For CdSe, two peaks located at 27.2° and 42° are attributed to the (101) and (110) planes of the hexagonal structure (JCPDS No. 00-008-0459) [15]. Similarly, the hexagonal phases of ZnS and ZnSe are confirmed by peaks at 25.7° and 48.8°, which correspond to the (100) and (103) planes (JCPDS No. 00-089-2940) [14]. These results collectively demonstrate the successful deposition and crystallization of CdS, CdSe, ZnS@Cu^{2+}, and ZnSe@Cu^{2+} quantum dots on the TiO_2 substrate.

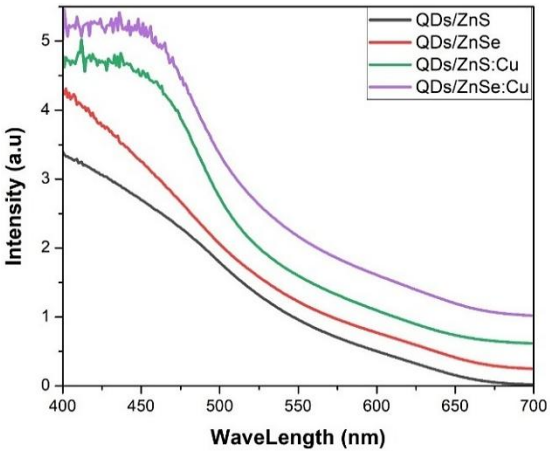

Figure 1. UV-Vis of X(S,Se) passivation layers doped - copper

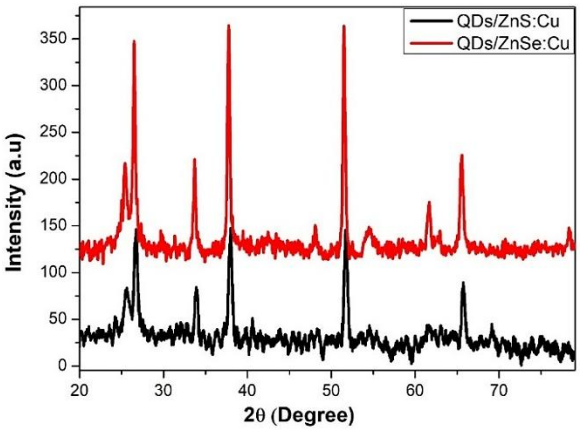

Figure 2. XRD spectra of X(S,Se):Cu passivation layers

The photovoltaic performance (J–V curves) of QDSSCs employing TiO_2/QDs/ZnS@Cu^{2+} and TiO_2/QDs/ZnSe@Cu^{2+} photoanodes was evaluated under standard solar illumination (100 mW·cm^{-2}), as summarized in Table 1 and Figure 3. The results indicate that the open-circuit voltage (Voc) and fill factor (FF) exhibit minimal variation between the two systems; however, the conversion efficiency shows a marked dependence on the current density. Specifically, the TiO_2/QDs/ZnS@Cu^{2+} photoanode yields a current density of 22 mA·cm^{-2} and a corresponding efficiency of 4.5%, which is lower than that of the TiO_2/QDs/ZnSe@Cu^{2+} counterpart. Upon Cu^{2+} doping into the ZnSe passivation layer, both the current density and power conversion efficiency are significantly enhanced, achieving values of 23 mA·cm^{-2} and 5.3%, respectively. This improvement is attributed to the substitution of Zn^{2+} by Cu^{2+} in the crystal lattice, which reduces the film's internal resistance and introduces impurity energy levels within the bandgap of ZnS and ZnSe, thereby enhancing photon absorption. These findings are in good agreement with previous studies, which demonstrated that Cu^{2+} and Mn^{2+} doping in ZnS substantially increased the photocurrent density.

This study examines the electron transfer mechanisms within thin-film layers, including electron transport at the photoanode interface (Rct2), electron diffusion in the electrolyte, and charge transfer at the cathode (Rct1), through electrochemical impedance spectroscopy (EIS) under illumination at 100 mW·cm^{-2}. The analysis, conducted using EC-LAB software, reveals that electrodes coated with Cu^{2+}-doped ZnS exhibit lower charge transfer resistances (Rct1 and Rct2) compared to those coated with Cu^{2+}-doped ZnSe, with minimum recorded values of Rct1 = 17 Ω and Rct2 = 33 Ω (Figure 4). Concurrently, the current density and overall device efficiency improved notably, from 22 mA·cm^{-2} to 23 mA·cm^{-2}. This enhancement is primarily attributed to the ZnS@Cu^{2+} layers, which not only improve photon absorption but also contribute to light reflection, thereby increasing the effective light harvesting by the TiO_2/QDs photoanode [17]-[22].

Furthermore, the conduction band edge of ZnS@Cu^{2+} is positioned higher than that of TiO_2/QDs, which helps suppress electron back diffusion and reduces recombination losses [23]. The incorporation of Cu^{2+} also induces a redshift in the absorption spectrum, extending into the visible light region, due to the formation of impurity levels within the bandgap of ZnS and ZnSe [24]. These results are consistent with the findings reported in previous studies, and demonstrate significantly improved efficiency compared to previous studies [8], [25].

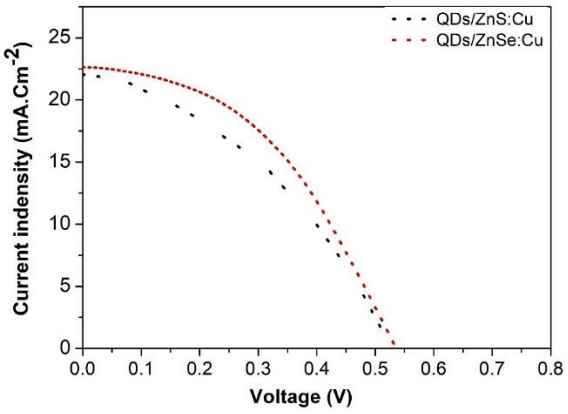

Figure 3. Photovoltaic performance of X(S,Se):Cu

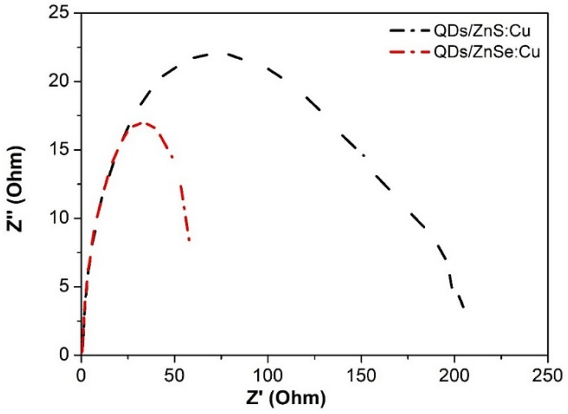

Figure 4. EIS of X(S,Se) passivation layers doped - copper

Table 1. The characteristic parameters of devices

Sample	V_{oc} (V)	J_{sc} (mA.cm^{-2})	FF	PCE (%)	R_{ct1} (Ω)	R_{ct2} (Ω)
Photoanode based ZnS:Cu	0.515	22	0.41	4.5	12	116
Photoanode based ZnSe:Cu	0.52	23.1	0.439	5.31	17	331

4. CONCLUSION

The Zinc(S,Se):Cu passivation layer was successfully synthesized via the SILAR method and employed to passivate the surfaces of CdS and CdSe quantum dots in the photoanode. Beyond its protective function, this layer enhances photon absorption in the quantum dot solar cell. The absorption spectrum shows a pronounced redshift in the visible region for the Zinc(S,Se):Cu-treated electrode compared with the undoped sample, consistent with the J–V characteristics. With this passivation layer, the current density increased to 23 mA/cm² and the power conversion efficiency reached 5.3%, confirming its contribution to

improved light harvesting. Electrochemical impedance spectroscopy further revealed that the Zinc(S,Se):Cu sample exhibits the lowest charge-transfer resistance, indicating suppressed recombination and more efficient electron transport. The structural features, surface morphology, and film thickness were verified by XRD and FESEM analyses.

FUNDING INFORMATION

Authors state no funding involved.

AUTHOR CONTRIBUTIONS STATEMENT

This journal uses the Contributor Roles Taxonomy (CRediT) to recognize individual author contributions, reduce authorship disputes, and facilitate collaboration.

Name of Author	C	M	So	Va	Fo	I	R	D	O	E	Vi	Su	P	Fu
Le Doan Duy	✓	✓	✓	✓	✓	✓		✓	✓	✓			✓	
Le Xuan Thuy			✓	✓	✓	✓	✓	✓	✓	✓	✓	✓		✓

C : **C**onceptualization
M : **M**ethodology
So : **So**ftware
Va : **Va**lidation
Fo : **Fo**rmal analysis
I : **I**nvestigation
R : **R**esources
D : **D**ata Curation
O : Writing - **O**riginal Draft
E : Writing - Review & **E**diting
Vi : **Vi**sualization
Su : **Su**pervision
P : **P**roject administration
Fu : **Fu**nding acquisition

CONFLICT OF INTEREST STATEMENT

Authors state no conflict of interest.

DATA AVAILABILITY

The data that support the findings of this study are available from the corresponding author, [LXT], upon reasonable request.

REFERENCES

[1] W. Shockley, "Problems related top-n junctions in silicon," *Czechoslovak Journal of Physics*, vol. 11, no. 2, pp. 81–121, Feb. 1961, doi: 10.1007/BF01688613.
[2] C. M. Nandanwar, N. S. Kokode, A. N. Yerpude, and S. J. Dhoble, "Effect of dopant concentration on luminescence properties of Ba3(PO4)2:RE (RE= Sm3+, Eu3+, Dy3+) phosphor for solid-state lighting," *Chemical Data Collections*, vol. 43, p. 100979, Feb. 2023, doi: 10.1016/j.cdc.2022.100979.
[3] C. M. Nandanwar, N. S. Kokode, A. V. Nande, A. N. Yerpude, R. S. Yadav, and S. J. Dhoble, "Photoluminescence studies of Sr3P4O13: Eu3+ phosphor prepared by wet chemical method: structural properties, charge compensation via alkali metal ions and Judd-Ofelt analysis," *Journal of Molecular Structure*, vol. 1322, p. 140224, Feb. 2025, doi: 10.1016/j.molstruc.2024.140224.
[4] C. M. Nandanwar, A. N. Yerpude, M. A. Patwardhan, N. S. Kokode, and R. L. Kohale, "Investigations on photoluminescence properties, quantum and Judd-Ofelt analysis of novel NaSrY(BO3)2:Eu3+ phosphor for lighting applications," *Materials Research Bulletin*, vol. 191, p. 113562, Nov. 2025, doi: 10.1016/j.materresbull.2025.113562.
[5] Y. Lee and Y. Lo, "Highly efficient quantum-dot-sensitized solar cell based on co-sensitization of CdS/CdSe," *Advanced Functional Materials*, vol. 19, no. 4, pp. 604–609, Feb. 2009, doi: 10.1002/adfm.200800940.
[6] R. D. Schaller, M. A. Petruska, and V. I. Klimov, "Effect of electronic structure on carrier multiplication efficiency: comparative study of PbSe and CdSe nanocrystals," *Applied Physics Letters*, vol. 87, no. 25, Dec. 2005, doi: 10.1063/1.2142092.
[7] M. C. Hanna, M. C. Beard, and A. J. Nozik, "Effect of solar concentration on the thermodynamic power conversion efficiency of quantum-dot solar cells exhibiting multiple exciton generation," *The Journal of Physical Chemistry Letters*, vol. 3, no. 19, pp. 2857–2862, Oct. 2012, doi: 10.1021/jz301077e.
[8] H. K. Jun and H. T. Tung, "A short overview on recent progress in semiconductor quantum dot-sensitized solar cells," *Journal of Nanomaterials*, vol. 2022, no. 1, Jan. 2022, doi: 10.1155/2022/1382580.
[9] J. Tyagi, H. Gupta, and L. P. Purohit, "Ternary alloyed CdS1−xSex quantum dots on TiO2/ZnS electrodes for quantum dots-sensitized solar cells," *Journal of Alloys and Compounds*, vol. 880, p. 160480, Nov. 2021, doi: 10.1016/j.jallcom.2021.160480.
[10] M. P. A. Muthalif, Y.-S. Lee, C. D. Sunesh, H.-J. Kim, and Y. Choe, "Enhanced photovoltaic performance of quantum dot-sensitized solar cells with a progressive reduction of recombination using Cu-doped CdS quantum dots," *Applied Surface Science*, vol. 396, pp. 582–589, Feb. 2017, doi: 10.1016/j.apsusc.2016.10.200.
[11] C. Xie *et al.*, "Core–shell heterojunction of silicon nanowire arrays and carbon quantum dots for photovoltaic devices and self-driven photodetectors," *ACS Nano*, vol. 8, no. 4, pp. 4015–4022, Apr. 2014, doi: 10.1021/nn501001j.
[12] A. Gupta and P. Bhargava, "Quantum dot sensitized solar cells".

[13] M. Alavi, R. Rahimi, Z. Maleki, and M. Hosseini-Kharat, "Improvement of power conversion efficiency of quantum dot-sensitized solar cells by doping of manganese into a ZnS passivation layer and cosensitization of zinc-porphyrin on a modified graphene oxide/nitrogen-doped TiO 2 photoanode," *ACS Omega*, vol. 5, no. 19, pp. 11024–11034, May 2020, doi: 10.1021/acsomega.0c00855.
[14] W. Zhu *et al.*, "Surface engineering boosting Al/Zn-coincorporated Cu–In–Se quantum dot-sensitized solar cell efficiency," *ACS Applied Energy Materials*, vol. 4, no. 6, pp. 5767–5774, Jun. 2021, doi: 10.1021/acsaem.1c00605.
[15] Z.-J. Mo *et al.*, "Observation of giant magnetocaloric effect under low magnetic field in Eu1−xBaxTiO3," *Journal of Alloys and Compounds*, vol. 694, pp. 235–240, Feb. 2017, doi: 10.1016/j.jallcom.2016.09.266.
[16] R. K. Chandrakar, R. N. Baghel, V. K. Chandra, and B. P. Chandra, "Synthesis, characterization and photoluminescence studies of Mn doped ZnS nanoparticles," *Superlattices and Microstructures*, vol. 86, pp. 256–269, Oct. 2015, doi: 10.1016/j.spmi.2015.07.043.
[17] N. Ullah, F. A. Jan, S. M. Shah, M. Usman, and M. H. Suliman, "Boosting efficiency of hybrid bulk heterojunction solar cells using organic dyes-grafted Sn-doped ZnS nanohybrid blended with P3HT," *Journal of Materials Science: Materials in Electronics*, vol. 36, no. 25, p. 1591, Sep. 2025, doi: 10.1007/s10854-025-15614-0.
[18] R. Beaulac *et al.*, "Spin-polarizable excitonic luminescence in colloidal Mn 2+ -doped CdSe quantum dots," *Nano Letters*, vol. 8, no. 4, pp. 1197–1201, Apr. 2008, doi: 10.1021/nl080195p.
[19] C. M. Nandanwar and N. S. Kokode, "Synthesis and photoluminescence properties of Ca5(PO4)3F: Ln (Ln: Dy3+, Eu3+ and Sm3+) phosphors for near UV-based solid state lighting," *Physics and Chemistry of Solid State*, vol. 23, no. 3, pp. 597–603, Sep. 2022, doi: 10.15330/pcss.23.3.597-603.
[20] J. Yu, Q. Xiang, and M. Zhou, "Preparation, characterization and visible-light-driven photocatalytic activity of Fe-doped titania nanorods and first-principles study for electronic structures," *Applied Catalysis B: Environmental*, vol. 90, no. 3–4, pp. 595–602, Aug. 2009, doi: 10.1016/j.apcatb.2009.04.021.
[21] N. T. P. Thu, B. Van Thang, and H. T. Tung, "Preparation of rGO-Cu2S for quantum dot sensitized solar cells application and investigation of its properties," *VNUHCM Journal of Natural Sciences*, vol. 6, no. 3, pp. 2271–2280, 2022.
[22] C. Zhai *et al.*, "One-pot synthesis of biocompatible CdSe/CdS quantum dots and their applications as fluorescent biological labels," *Nanoscale Research Letters*, vol. 6, no. 1, p. 31, Sep. 2010, doi: 10.1007/s11671-010-9774-z.
[23] N. Firoozi, H. Dehghani, M. Afrooz, and S. S. Khalili, "Improvement photovoltaic performance of quantum dot-sensitized solar cells using deposition of metal-doped ZnS passivation layer on the TiO2 photoanode," *Microelectronic Engineering*, vol. 198, pp. 8–14, Oct. 2018, doi: 10.1016/j.mee.2018.06.007.
[24] H. N. Phuong, T. Van Man, H. T. Tung, H. K. Jun, B. Van Thang, and L. Q. Vinh, "Effect of precursors on Cu2S counter electrode on the quantum dot sensitized solar cell performance," *Journal of the Korean Physical Society*, vol. 80, no. 12, pp. 1133–1142, Jun. 2022, doi: 10.1007/s40042-022-00460-8.
[25] S. C. Poh, H. Ahmad, C. H. Ting, H. T. Tung, and H. K. Jun, "Performances of flexible dye-sensitized solar cells fabricated with binder-free nanostructure TiO2," *Journal of Materials Science: Materials in Electronics*, vol. 32, no. 9, pp. 12031–12041, May 2021, doi: 10.1007/s10854-021-05833-6.

BIOGRAPHIES OF AUTHORS

Le Doan Duy received the master degree in physics from Can Tho University, Vietnam. He is working as a lecturer at the Faculty of Basic Sciences, Vinh Long University of Technology Education, Vietnam. His research interests focus on developing the patterned substrate with micro and nano-scale to apply for physical and chemical devices such as solar cells, OLED, photoanode, and theory physics. He can be contacted at email: duyld@vlute.edu.vn.

Le Xuan Thuy received the master degree in physics from Can Tho University, Vietnam. She received a Ph.D. from the Vietnam Academy of Science and Technology. She is working as a lecturer at the Faculty of Basic Sciences, Vinh Long University of Technology Education, Vietnam. Her research interests: solar cells, OLED, photoanode, and theory physics. She can be contacted at email: thuylx@vlute.edu.vn.